Journal of Macromolecular Science, Part A
Publication details, including instructions for authors and subscription information:
http://www.informaworld.com/smpp/title~content=t713597274

Chitosan Based Scaffolds by Lyophilization and sc.CO_2 Assisted Methods for Tissue Engineering Applications

Kumari Rinki[a]; P. K. Dutta[a]
[a] Department of Chemistry, M. N. National Institute of Technology, Allahabad, India

Online publication date: 05 April 2010

To cite this Article Rinki, Kumari and Dutta, P. K.(2010) 'Chitosan Based Scaffolds by Lyophilization and sc.CO_2 Assisted Methods for Tissue Engineering Applications', Journal of Macromolecular Science, Part A, 47: 5, 429 — 434
To link to this Article: DOI: 10.1080/10601321003659630
URL: http://dx.doi.org/10.1080/10601321003659630

Journal of Macromolecular Science, Part A: Pure and Applied Chemistry (2010) **47**, 429–434

ISSN: 1060-1325 print / 1520-5738 online
DOI: 10.1080/10601321003659630

Taylor & Francis
Taylor & Francis Group

Chitosan Based Scaffolds by Lyophilization and sc.CO_2 Assisted Methods for Tissue Engineering Applications

KUMARI RINKI and P. K. DUTTA*

Department of Chemistry, M. N. National Institute of Technology, Allahabad, India

Received August 2009, Accepted October 2009

Porous chitosan scaffolds with possible tissue engineering applications were synthesized by using lyophilization and supercritical carbon dioxide (sc.CO_2) drying technique. 1% Chitosan (CS) solution in aq. acetic acid was treated with 37% formaldehyde solution; the resulting hydrogels were subjected to solvent-exchange prior to the final treatment procedures. Their morphology, pore structure, and physical properties were characterized by Fourier transform infrared spectroscopy (FTIR), thermal analysis, scanning electron microscopy (SEM), transmission electron microscopy (TEM) and the specific surface areas and porosities of scaffolds were determined by using N_2 adsorption. The sc.CO_2 treated scaffolds showed a much greater surface area in comparison to the lyophilized one. Hence, sc.CO_2 treated scaffolds is better for cell proliferation. We further investigated the bioactivity of sc.CO_2 treated scaffolds using simulated body fluid (SBF). The sc.CO_2 assisted chitosan scaffold prepared by using green chemistry approach is highly pure and from a hygienic point of view, it is an ideal material for tissue engineering applications.

Keywords: Chitosan, scaffolds, lyophilization, sc.CO_2, tissue engineering

1 Introduction

Chitosan is a cationic polymer derived from chitin comprising copolymers of $\beta(1\rightarrow4)$-glucosamine and N-acetyl-D-glucosamine. Chitin is a natural-origin polysaccharide, found in crustacean shells and is the second most abundant polymer found widely after cellulose. Chitosan shows excellent physicochemical and biological properties which make it an ideal material for the preparation of drug delivery systems and for tissue engineering applications (1). Chitosan, a copolymer of glucosamine and N-acetylglucosamine, is a biomaterial with antiseptic, bioactive, and biocompatible properties (2). The protonation of the amino groups on the chitosan molecules led to dissolution in organic acid at low pH value. The amino groups can be utilized for coupling chitosan with other biomolecules (3). Chitosan has been fabricated in several forms to be used in tissue engineering applications, namely, membranes (4), particles (5), fibers and 3D fiber meshes (6); tissue engineering involves the repair and regeneration of damaged tissue. The paradigm of tissue engineering consists of seeding cells on a suitable scaffold which serves as a substrate for initial cell attachment and as a physical support to guide neo-tissue formation (7–10). One of the major strategies in tissue engineering is to enable the self-healing potential of the patient to regenerate body tissue and organs (11,12). This goal can be achieved if a bioactive scaffold is designed in such a manner that at the same time it provides cells a support to grow and also induces their differentiation and proliferation. The important issue in tissue engineering is scaffolding. In tissue engineering applications, the cationic nature of chitosan is primarily responsible for electrostatic interactions with anionic glycosaminoglycans, proteoglycans and other negatively charged molecules. This property plays an important role in tissue engineering applications because a large number of cytokines/growth factors are linked to glycosaminoglycans, and a scaffold incorporating a chitosan–glycosaminoglycans complex may retain and concentrate growth factors secreted by any colonizing cells. Moreover, the N-acetylglucosamine moiety in chitosan is active in the specific interactions with growth factors, receptors, and adhesion of proteins (13). Chitosan is composed of glucosamine (GS) which is similar to the component of HA in extracellular matrix (ECM) and can be degraded into CS oligomers or GS, which can be metabolized (14). A number of scaffolds fabrication methods have been suggested by various researchers' viz. electrospinning, salt leaching, solid free form fabrication, phase separation (14–17). These fabrication techniques involve the use of organic solvents that may remain at a high level for some polymer formulations. Since organic solvents are toxic to cells, the residual solvents must be removed to comply with the FDA

*Address correspondence to: P. K. Dutta, Department of Chemistry, M. N. National Institute of Technology, Allahabad 211004, India. Tel.: 91-532-2271272; Fax: 91-532- 2545341; E-mail: pkd_437@yahoo.com

regulations (18). Recently, some of the researchers had prepared scaffolds by using supercritical carbon dioxide (19, 20). It has been reported that sc.CO_2serves as a promising process medium for fabrication of tissue engineering scaffolds (18, 21–25). A high purity product, free of residual solvents is obtained, since no organic solvents are involved in the fabrication process. Supercritical carbon dioxide (sc.CO_2) has been identified as prime candidates to develop alternative clean processes for the preparation of tissue engineering scaffolds (1). In the present study, we made a comparative study of scaffolds prepared by two different methods, viz. sc.CO_2 drying and lyophilization technique. The bioactive nature of the sc.CO_2 treated scaffolds will be evaluated by analyzing the biomimetic apatite formation on the scaffolds during immersion in simulated body fluid (SBF).

2 Experimental

2.1 Materials

Chitosan (79% deacetylated) was purchased from India Sea Food Pvt. Ltd., Kochi, India, Acetic Acid; Merck, Formaldehyde (37% aqueous); Merck. Carbon dioxide (CO_2) 99.9% purity was sourced from BOC Ltd. and used as such.

2.2 Sample Preparation

0.2 M solution of chitosan was prepared by using 1% aq. acetic acid and the crosslinker, 37% formaldehyde solution was added slowly to the chitosan solution in the stirring condition. Stirring was continued until the solution will be turned into viscous gel. Then the prepared hydrogel was subjected to solvent exchange into acetone, a further two exchanges were undertaken to remove water from the structure.

2.3 Freeze-drying (Lyophilization)

The hydrogel, after its subjection to solvent exchange in acetone, was kept at −20°C for 24 h in a deep freezer and lyophilized in a freeze-drier and then the sample was kept in vacuum desiccators for its further study.

2.4 Supercritical Fluid (SCF) Drying

After solvent exchange, the chitosan-formaldehyde derivative was placed inside a sealed chamber of Thar SFE 500 sc.CO_2 extractor. The temperature and pressure were raised to 40°C and 200 bar, respectively. The reaction was left for 2 h and a flow of $CO_2$was then applied through the sample in order to replace all the organic solvent with CO_2. The pressure was then released slowly to the atmosphere and the temperature was reduced to 20°C.

2.5 Bioactivity Studies

The bioactivity studies of sc.CO_2 treated scaffolds were carried out by a biomimetic method with 1.5 X SBF solutions (26–28). The sc.CO_2 scaffolds were soaked in 30 ml of a SBF at 36°C for 7, 14 and 21days. The SBF solution was prepared by the following method (29), and contained 15 ml of each of the following: 2.74 mol L^{-1} NaCl, 0.06 mol L^{-1} KCl, 0.05 mol L^{-1} CaCl2, 0.03 mol L^{-1} MgCl2, 0.0895 mol L^{-1} NaHCO3, 0.02 mol L^{-1} K2HPO4 and 0.01 mol L^{-1} Na2SO4. These were added to a 200 ml volumetric flask along with 25 ml each of 0.4 mol L^{-1} Tris hydroxy methyl methane amine and 0.36 mol L^{-1} of HCl. The pH of the solution was adjusted to 7.4 by adding a few drops of HCl with the remainder of the volume being distilled water.

2.6 Characterization

The scaffolds were characterized by means of a FTIR technique (Bruker ATR), differential thermogravimetric (DTG) and thermogravimetric analysis (TGA) with STA 600 thermal analyzer, scanning electron microscopy (SEM) and transmission electron microscpoy (TEM) with Jeol electron microscopy. The Brunauer-Emmett-Teller (BET) surface area was calculated using nitrogen adsorption data in the BET region ($P/P_0 \leq 0.3$). The BET equation was used for the calculation of the specific surface area and the pore size distribution. The pore size distribution of the sample was determined by the Barret-Joiner-Halenda(BJH) method. The total pore volume of the sample was calculated on the basis of the amount of nitrogen adsorbed at a relative pressure of about 0.97. The nitrogen adsorption isotherms were measured at liquid nitrogen temperature (77 K) using a Micromeritics ASAP 2010 system after degassing the sample.

3 Results and Discussion

The preparation of the chitosan-formaldehyde derivative is shown in Scheme 1. The hydrogel was subjected to solvent exchange to remove water and thus formation of aerogel by the use of sc.CO_2 with the retaining of microstructures is designated as scaffolds. However, the freeze-drying results in the formation of cryogel.

3.1 SCF and Freeze-drying Processing

SCF processing of the Schiff base resulted into a light pink, solid material, and by this method, the texture remained after drying. In this method, the processing solvent CO_2 is above the critical point, there is no interface, hence no meniscus tension; so the aerogel keeps the structure of the hydrogel, leading to a very high porosity by

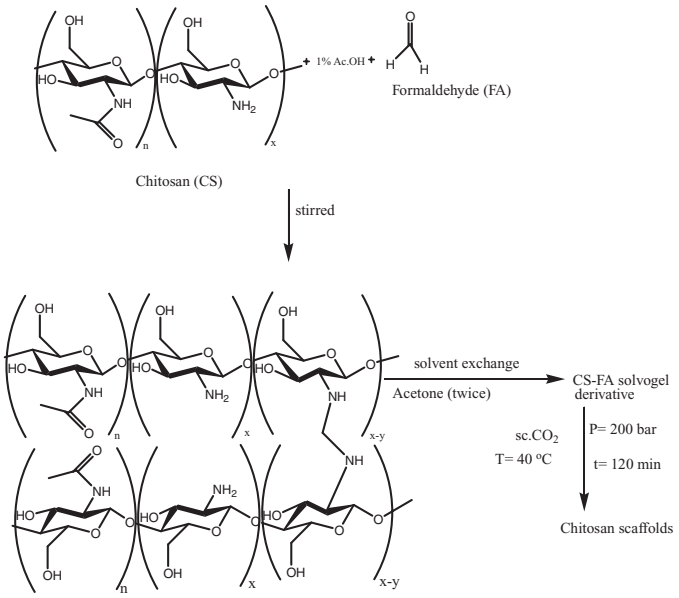

Sch. 1. Preparation of chitosan scaffolds by sc. CO_2 treatment.

dispersion of the nanometric polysaccharide fibrils that form the aerogel scaffold (30). The freeze-drying of chitosan derivative also resulted into a porous, light pink, solid material.

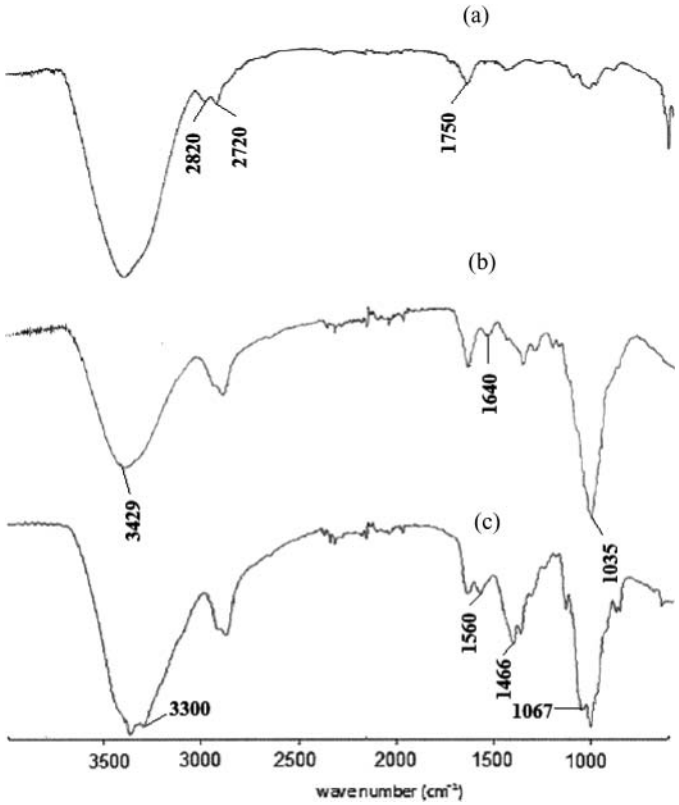

Fig. 1. FTIR spectra of (a) chitosan; (b) formaldehyde and (c) chitosan-formaldehyde derivative.

3.2 FTIR Spectroscopy

The prominent peaks of chitosan are (Fig. 1b) 3429 cm^{-1} (O–H stretch overlapped with N–H stretch), 2921 and 2867 cm^{-1} (C–H stretch), 1640 cm^{-1} (amide II band, C=O stretch of acetyl group), 1592 cm^{-1} (amide II band, N–H stretch) 1485–1380 cm^{-1} (asymmetric C–H bending of CH_2 group) and 1035 cm^{-1} (bridge O stretch) of glucosamine residue. The characteristic peaks of formaldehyde (Fig. 1a) are located at 1750 cm^{-1} for the carbonyl group and one near 2820 cm^{-1} for C–H asymmetric stretching and the other near 2720 cm^{-1} for C–H symmetric stretching. In the IR spectra of chitosan derivative, the strong peak at 1466 cm^{-1} may be assigned to the asymmetric deformation of CH_2, and the C=O adsorption peak of secondary hydroxyl groups which become stronger and move to 1067 cm^{-1}; the intensity of primary alcohol 1035 cm^{-1}due to C=O stretching vibration, becomes much smaller than in chitosan. Chitosan-formaldehyde derivative (Fig. 1c) shows a significant peak at 1560 cm^{-1} due to the formation of a crosslink from an initial formation if imine between the amino group of one chain and formaldehyde, followed by

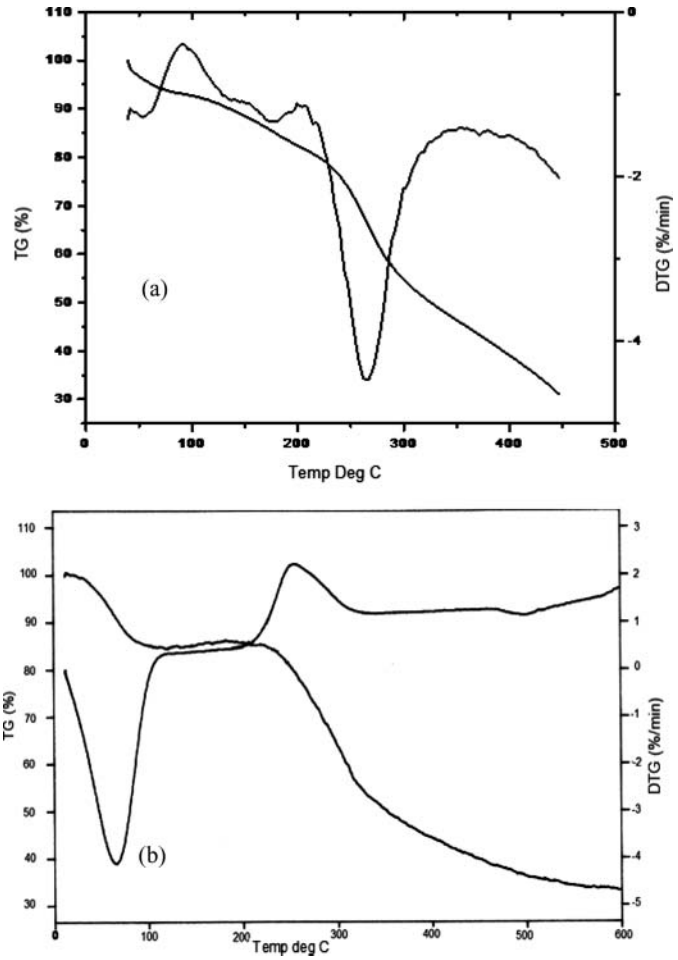

Fig. 2. TGA and DTG of (a) lyophilized chitosan scaffolds and (b) sc.CO_2 treated chitosan scaffolds.

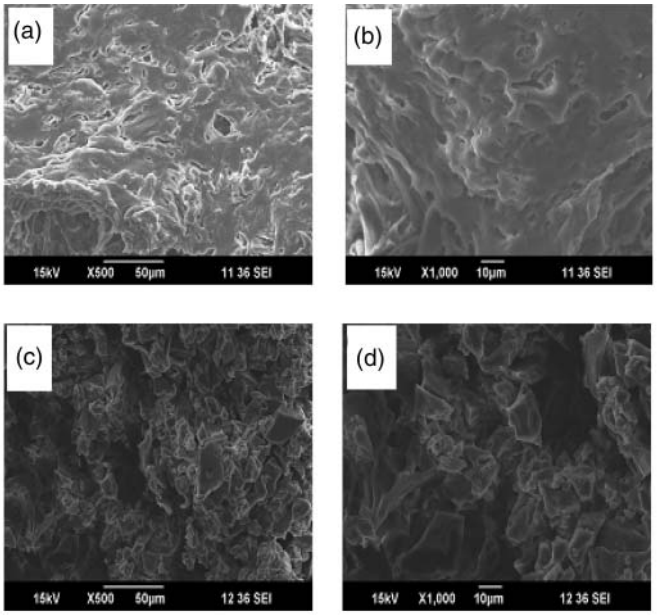

Fig. 3. SEM images of (a) and (b): lyophilized chitosan scaffolds; (c) and (d): sc.CO_2 treated chitosan scaffolds.

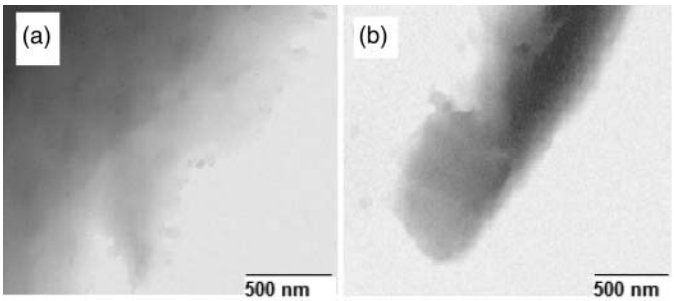

Fig. 4. TEM images of (a): lyophilized chitosan derivative and (b): sc. CO_2 treated chitosan derivative.

a subsequent reaction with a second amino group in a different chain, leading to the –NH-CH_2-NH- unit (31). The band at 1560 cm^{-1} is ascribed to the new NH deformation of this group, and additional activity around 3300 cm^{-1} is possibly due to the NH stretching of the same group. This characteristic peak confirms the formation of crosslinks (shown in Scheme 1) after the reaction of chitosan with formaldehyde.

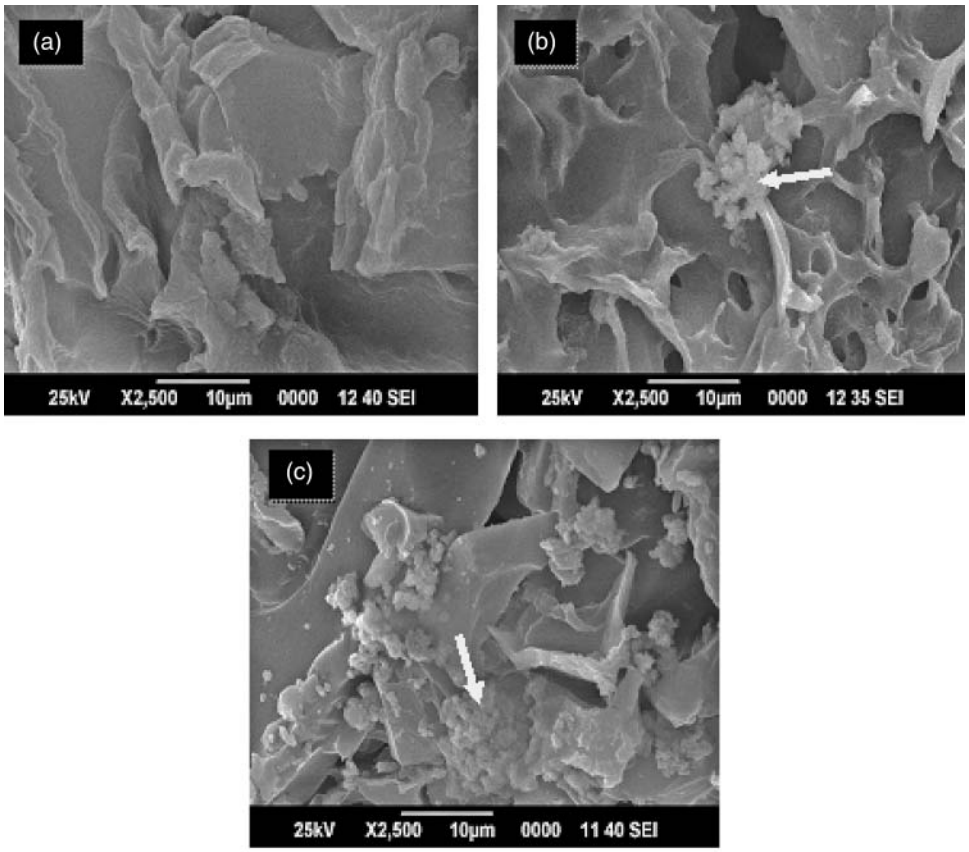

Fig. 5. SEM images of sc.CO_2 treated chitosan scaffold showing formation of apatite (shown by arrow) after immersion in SBF for (a): 7 days; (b): 14 days and (c): 21 days.

3.3 Thermal Analysis

The TGA curve of lyophilized scaffolds, represented in Figure 2a shows that the chitosan has two main decomposition stages with the first occurring in the range of 36°–100°C, and is attributed to the evaporation of water with a weight loss of about 10%. The primary degradation of chitosan started at about 231°C and completely degraded at about 446°C. The DTG curve (Fig. 2a) of the lyophilized scaffolds shows single stage degradation. The temperature of initial degradation (T_1) of chitosan was about 205°C and the temperature of the maximum rate of degradation (T_{1max}) was about 265°C; finally a high char residue of about 31 wt% was produced at 446°C.

The TGA curve of scaffolds obtained after sc.CO_2 drying represented in Figure 2b shows that the chitosan derivative has two main decomposition stages with the first occurs in the range of 50°–100°C, attributed to the evaporation of water with a weight loss of about 15%. The primary degradation of chitosan started at about 220°C and completely degraded at about 600°C. In spite of the water loss, the TG curves indicate that chitosan scaffolds underwent a single stage of degradation. However, the DTG curve (Fig. 2b) shows an endothermic peak at 80°C which is attributed to the evaporation of water from the chitosan scaffold and the temperature of maximum rate of degradation was about 255°C; finally a high char residue of about 28% was produced at 600°C. The DTG curves show two peaks, which were considered to indicate the temperature of the maximum rate of the first and second degradation stages. These results suggest that the scaffolds obtained after sc.CO_2 drying is thermally more stable in comparison to the lyophilized one.

3.4 Morphology

The scanning electron micrographs (SEMs) of the sc. CO_2treated scaffolds are shown in Figure 3. The SEMs of chitosan derivative exhibited a polyphasic microporous structure. The pore dimensions are non-uniform with thin walls. However, the SEM images of lyophilized chitosan scaffolds also reveal a porous structure with interconnected pores. Both types of treatment result in a porous scaffold.

The transmission electron microscopy (TEM) provides us the information about the morphology in detail. The TEM images as shown in Figure 4a of sc. CO_2 treated chitosan derivative showed a porous material with uniform pore structures and shapes of the particles are homogeneous (32). However, the lyophilized one showed a less porous material and shapes of the particles are not homogeneous which is shown in Figure 4b.

3.5 Porosimetry Measurement

Scaffolds' surface morphology plays an important role in angiogenesis. Scaffolds having good surface area will be better for cell attachment and proliferation (19). The Brunauer-Emmett-Teller (BET) surface area was calculated using adsorption data in the BET region ($P/P_0 \leq 0.3$). The pore size distribution of the chitosan derivative was determined from desorption branches of the isotherms by the Barret-Joiner-Halenda (BJH) method. The BJH pore size is defined as the maximum of the BJH pore size distribution [33].The sc. CO_2 treated chitosan derivative demonstrated a BET surface area of 135 m^2g^{-1}, with a BJH total pore volume of 0.51 cm^3g^{-1} and an average pore diameter (4V/A by BET) of 10.8 nm. However, the BJH cumulative surface area is found to be 2.19 m^2g^{-1} and BJH average pore diameter is 0.47 nm for lyophilized chitosan derivative. For the lyophilized chitosan derivative, the surface area as well as the pore diameter is very less in comparison to the sc.CO_2 treated chitosan derivative. In this way, the scaffolds prepared by sc.CO_2 treatment serves the purpose better than the lyophilized one.

3.6 Bioactivity Studies

The bioactivity studies of sc.CO_2 treated chitosan scaffolds were carried out by using 1.5X SBF and characterized by

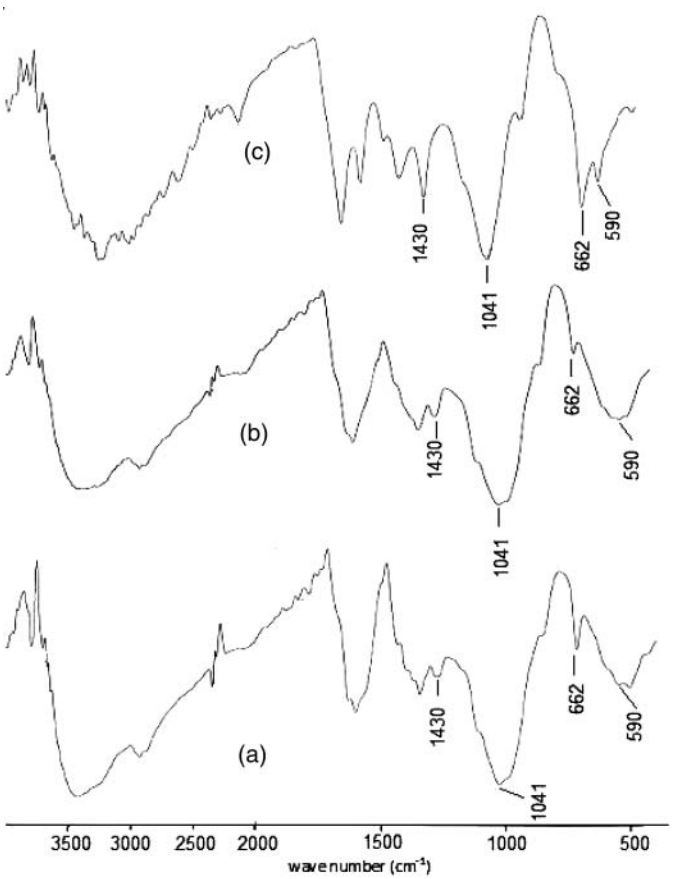

Fig. 6. FTIR spectra of sc.CO_2 treated scaffolds soaked in SBF after immersion in SBF for (a): 7 days; (b): 14 days and (c): 21 days.

means of SEM and FTIR. Figure 5 shows the SEM images of sc.CO_2 treated chitosan scaffolds after immersion for 7, 14 and 21 days in SBF solution. The SEM images show the formation of calcium phosphate apatite layer on the surface of sc.CO_2 treated chitosan scaffolds after immersion in SBF, and these deposits grew in size with increasing soaking time.

Figure 6 shows the FTIR spectrum of sc.CO_2 treated chitosan scaffolds after immersion for 7, 14 and 21 days in 1.5 X SBF solutions. FTIR results also confirm the apatite nature of the mineral layer as previously observed by SEM analysis. The adsorption peak between 1041 and 590 cm^{-1}can be assigned to the ν_3 P–O stretching and ν_4 bending mode of the phosphate, respectively. The strong adsorption band at 662 cm^{-1} corresponds to the PO_4 vibrations. The peaks at 1430 cm^{-1} were due to the calcium phosphate. These results confirmed the formation of calcium phosphate on the scaffolds after immersion in SBF solution and confirmed the bioactivity of the scaffolds.

4 Conclusions

The chitosan scaffolds prepared by sc.CO_2 treatment is highly porous and it has greater pore size and surface area in comparison to the lyophilized one and is expected for better cell proliferation. The sc.CO_2 treated chitosan scaffolds showed apatite formation, hence can be applicable in tissue engineering. Moreover, the use of sc.CO_2as the reaction medium made it highly pure and from biomedical application point of views (especially, hygienic) the green chemistry approach is a benign technique.

Acknowledgments

The authors thank the Commonwealth Scholarship Commission-London for providing Academic Staff Fellowship Award-2007 to PKD and KR is thankful to Professor Arun B. Samaddar, Director, MNNIT, Allahabad for providing her institute fellowship.

References

1. Duarte, A.R.C., Mano, J.F. and Reis, R.L. (2009) *Eur. Polymer J.,* 45(1), 141–148.
2. Rhoades, J. and Roller, S. (2000) *Appl. Environ. Microbiol.,* 66(1), 80–86.
3. Santos, T.C., Marques, A.P., Silva, S.S., Oliveira, J.M., Mano, J.F., Castro, A.G. and Reis, R.L. (2007) *J. Biotechnol.,* 132(2), 218–226.
4. Prabaharan, M. and Mano, J.F. (2005) *Drug Delivery*, 12(1), 41–57.
5. Tuzlakoglu, K., Alves, C.M., Mano, J.F. and Reis, R.L. (2004) *Macromol. Biosci.* 4(8), 811–819.
6. Hutmacher, D.W. (2000) *Biomaterials*, 21(24), 2529–2543.
7. Yang, S.F., Leong, K.F., Du, Z.H. and Chua, C.K. (2001) *Tissue Eng.,* 7(6), 679–689.
8. Chen, G.P., Ushida, T. and Tateishi,T. (2002) *Macromol. Biosci.*, 2(2), 67–77.
9. Salgado, A.J., Coutinho, O.P. and Reis, R.L. (2004) *Macromol. Biosci*., 4(8), 743–765.
10. Malafaya, P.B., Silva, G.A., Baran, E.T. and Reis, R.L. (2002) *Curr. Opin. Solid State Mater. Sci.*, 6(4), 283–295.
11. Malafaya, P.B., Silva, G.A. and Reis, R.L. (2007) *Adv. Drug Del. Rev.,* 59(4–5), 207–233.
12. Mano, J.F., Hungerford, G. and Ribelles, J.L.G. (2008) *Mater. Sci. Eng. C,* 28(8), 1356–1365.
13. Wang, J., Chen, Y., Ding, Y., Shi, G. and Wan, C. (2008) *Appl. Surface Sci.,* 255(2), 260–262.
14. Shalumon, K.T., Binulal, N.S., Selvamurugan, N., Nair, S.V., Menon, D., Furuike, T., Tamura, H. and Jayakumar, R. (2009) *Carbohydr. Polymers,* 77(4), 863–869.
15. Murphy, W.L., Dennis, R.G., Kileny, J.L. and Mooney, D.J. (2002) *Tissue Eng.,* 8(1), 43–52.
16. Leong, K.F., Cheah, C.M. and Chua, C.K. (2003) *Biomaterials,* 24(13), 2363–2378.
17. Chen, V.J., Ma, P.X. *Polymer Phase Separation*. In: Scaffolding in Tissue Engineering, Ma, P.X. and Elisseeff, J., Eds. CRC Press, Taylor & Francis Group, USA. 2006, p. 125–140.
18. Hu, X. and Lessery, A.J. (2006) *J. Cellular Plastics*, 42(6), 517–527.
19. Rinki, K.,Dutta, P.K., Hunt, A.J., Clark, J.H. and Macquarrie, D.J. (2009) *Macromol. Symp.,* 277(1), 36–42.
20. Tsivintzelis, I., Pavlidou, E. and Panayiotou, C. (2007) *J. Supercritical Fluids,* 40(2), 317–322.
21. Shi, C., Huang, Z., Kilic, S., Xu, J., Enick, R.M., Beckman, E.J., Carrm, A.J., Melendez, R.E. and Hamilton, A.D. (1999) *Science*, 286 (5444), 1540–1543.
22. Goel, S.K. and Beckman, E.J. (1994) *Polymer Eng. Sci.,* 34(14), 1137–1147.
23. Arora, K.A., Lesser, A.J. and McCarthy, T.J. (1999) *Macromolecules,* 32(8), 2562–2568.
24. Mooney, D.J., Baldwin, D.F., Suh, N.P., Vacanti, J.P. and Langer, R. (1996) *Biomaterials,* 17(14), 1417–1422.
25. Sheridan, M.H., Shea, L.D., Peters, M.C. and Mooney, D.J. (2000) *J. Control Release,* 64(1–3), 91–102.
26. Rinki, K. and Dutta, P.K. (2010) *Int. J. Biologi. Macromol.*, 46(2), 261–266.
27. Jayakumar, R., Divya Rani, V.V., Shalumon, K.T., Sudheesh Kumar P.T., Nair, S.V., Furuike, T. and Tamura, H., (2009) *Asian Chitin J.* 5(1), 63–70.
28. Kong, L., Gao Y., Lu, G., Gong, Y., Zhao, N. and Zhang, X. (2006) *Eur. Polym. J.* 42(12), 3171–3179.
29. Oyane, A., Kim, H.M., Furuya, T., Kokubo, T., Miyazaki, T. and Nakamura, T. (2003) *J. Biomed. Mater. Res.,* 65A(2), 188–195.
30. Kadib, A.E., Molvinger, K., Guimon, C., Quignard, F. and Daniel, B. (2008) *Chem. Mater.,* 20(6), 2198–2204.
31. Singh, A., Dutta, J., Chattopadyaya, M.C., Dutta, P.K. 2004, Synthesis and optimization of water uptake efficiency of chitosan hydrogels cross-linked with formaldehyde. In: Proceedings of PSM-PAF National Seminar Polymer Research in India Opportunity & Challenges, India. Dutta P.K., Ed. p. 88–95.
32. Hwang, C.S. and Cho, I.H. (2005) *Bull. Korean Chem. Soc.,* 26(11), 1776–1782.
33. Pandya, P.H., Jasra, R.V., Newalkar, B.L. and Bhatt, P.N. (2005) *Micro Meso Mater.,* 77(1), 67–77.